Multilevel Simulation for the Investigation of Fast Diffusivity Paths

H. Ceric*†, R. L. de Orio*†, F. Schanovsky*†, W. H. Zisser*, and S. Selberherr*
*Institute for Microelectronics, TU Wien, Gußhausstraße 27–29/E360, A-1040 Wien, Austria
†Christian Doppler Laboratory for Reliability Issues in Microelectronics
Email: ceric@iue.tuwien.ac.at

***Abstract*—The reliability of interconnects in modern integrated circuits is determined by the magnitude and direction of the effective valence for electromigration (EM). The effective valence depends on local atomistic configurations of fast diffusivity paths such as metal interfaces, dislocations, and the grain boundary; therefore, microstructural variations lead to a statistically predictable behavior for the EM life time. Quantum mechanical investigations of EM have been carried out on an atomistic level in order to obtain numerically efficient methods for calculating the effective valence. The results of *ab initio* calculations of the effective valence have been used to parameterize the continuum-level electromigration model and the kinetic Monte Carlo model. The impact of fast diffusivity paths on long term EM behavior is demonstrated with these models.**

I. Introduction

Electromigration (EM) experiments indicate that the copper interconnect lifetime decreases with every new interconnect generation. In particular, fast diffusivity paths cause a significant variation in the interconnect performance and EM degradation [1]. In order to produce reliable interconnects, the fast diffusivity paths must be addressed when introducing new designs and materials. The EM lifetime depends on a variation of material properties at the microscopic and atomistic levels. Microscopic properties are grain boundaries and grains with their crystal orientation [2]. Atomistic properties are configurations of atoms at the grain boundaries, at the interfaces to the surrounding layers, and at the cross-section between grain boundaries and interfaces. Modern Technology Computer-Aided Design (TCAD) tools, in order to meet the challenges of contemporary interconnects, must cover two major areas: physically based continuum-level modeling and first-principle/atomistic-level modeling. A multilevel modeling and simulation approach is presented in order to investigate the impact of fast diffusivity paths on EM reliability.

II. Theoretical Background

The source of EM performance variation lies in the atomistic level, for which analyse using first-principle methods must be employed. The crucial parameters to determine EM behavior is the effective valence which strongly differs between bulk, grain boundaries, dislocations, and interfaces. In general, the effective valence is a tensor field ($\bar{Z}$), defined as a linear relationship between the EM force ($\vec{F}$) and an external electric field $\vec{E}$.

$$\vec{F}(\vec{R}) = e\bar{Z}(\vec{R})\vec{E} \tag{1}$$

In order to calculate the effective valence several methods have been proposed, all of which implement a calculation of electron scattering states [3]. Density functional theory (DFT), in connection with the augmented plane wave (APW) method [4] or the Korringa-Kohn-Rostoker (KKR) [5] method, has been established as a powerful method for the determination of scattering states while requiring a demanding computational scheme. The cumbersome representation of scattering wave functions with many parameters represents a heavy burden on the stability and the accuracy of subsequent numerical steps. However, it is possible to apply a more robust and efficient method to calculate the effective valence which relies only on the electron density $\rho(\vec{k}, \vec{r})$.

A. Electronic Density Based Calculation of Effective Valence

Using the Born-Oppenheimer approximation, the force, $F(\vec{R})$, exerted by the electron gas on an atom situated at $\vec{R}$, may be written as [6], [7], [8]

$$F(\vec{R}) = \sum_{\vec{k}} g(\vec{k}) \langle \psi_{\vec{k}}(\vec{r}) | - \nabla_{\vec{R}} V(\vec{r} - \vec{R}) | \psi_{\vec{k}}(\vec{r}) \rangle \tag{2}$$

where V is the interaction potential between an electron and the migrating atom, $\psi_k(\vec{r})$ are the scattering states for electrons in the absence of an external electric field, and $g(\vec{k})$ is the shifted electron distribution which has the form

$$g(\vec{k}) = e\tau(\vec{k})\vec{v}(\vec{k}) \cdot \vec{E}\, \frac{\partial f_0}{\partial \mathcal{E}_{\vec{k}}}. \tag{3}$$

Here, f_0 is the equilibrium electron distribution, $\tau(\vec{k})$ is the relaxation time due to scattering by phonons, and $v(\vec{k})$ is the electron group velocity. In the low temperature limit

$$\frac{\partial f_0}{\partial \mathcal{E}_{\vec{k}}} = -\delta(\mathcal{E}_F - \mathcal{E}_{\vec{k}}). \tag{4}$$

and (2) is then re-written in the form

$$\begin{aligned} \vec{F}(\vec{R}) = \frac{e\Omega}{4\pi^3} \iiint d^3\vec{k}\, \delta(\mathcal{E}_F - \mathcal{E}_{\vec{k}}) \tau(\vec{k}) [\vec{v}(\vec{k}) \cdot \vec{E}] \cdot \\ \cdot \iiint_{\mathrm{EZ}} d^3\vec{r}\, \psi_k^*(\vec{r}) \nabla_{\vec{R}} V(\vec{R} - \vec{r}) \psi_k(\vec{r}). \end{aligned} \tag{5}$$

Ω is the volume of a unit cell. The first integration is over the k-space and the second over the volume of the crystal. By taking into account (1) and

$$\rho(\vec{k}, \vec{r}) = |\psi_k(\vec{r})|^2 \tag{6}$$

978-1-61284-418-3/11/$26.00 © 2011 IEEE

components of the effective valence tensor $\bar{Z}$ are expressed as

$$Z_{i,j}(\vec{R}) = \frac{\Omega}{4\pi^3} \iiint d^3\vec{k}\, \delta(\mathcal{E}_F - \mathcal{E}_{\vec{k}})\tau(\vec{k})[\vec{v}(\vec{k}) \cdot \hat{x}_j] \cdot \\ \cdot \iiint d^3\vec{r}\, \rho(\vec{k},\vec{r})[\nabla_{\vec{R}} V(\vec{R}-\vec{r}) \cdot \hat{x}_i], \quad i,j = x,y. \tag{7}$$

For the calculation of the electron density the DFT tool VASP [9] was used. An example of a VASP calculation is presented in Fig. 1. The electron density alone provides a qualitative explanation for the fact that the effective valence is higher in the bulk than in the grain boundaries. Similar analyses can be performed for atomic structures of different copper/insulator interfaces. Higher electron densities lead to higher effective valences, as can be seen from (7).

B. Jellium Model of Grain Boundary

The electric potential calculated with DFT is also applied for a simple jellium model. Here, the grain boundary is represented as a repulsive potential barrier for current carrying electrons. In this case the evaluation of integral (7) is not necessary, since only a simple one-dimensional barrier problem must be dealt with, e.g. the precisely calculated DFT repulsive potential is approximated with a rectangular barrier potential. To estimate the value of the effective valence, both inside the grain boundary and in the copper bulk, an external electric field parallel to the grain boundary must be applied, obtaining the two-dimensional potential (cf. Fig. 2). Current carrying electrons are now described with the two-dimensional Schrödinger equation

$$\frac{\hbar}{2m}\Delta_{x,y}\psi(x,y) + V(x,y)\psi(x,y) = \mathcal{E}\psi(x,y). \tag{8}$$

The two-dimensional potential can be separated into a component for the barrier $V(x)$ and a component due to the external electric field $V(y)$

$$V(x,y) = V(x) + V(y). \tag{9}$$

In this case, the solution of the two-dimensional Schrödinger equation is represented as a product of two one-dimensional solutions [10]

$$\psi(x,y) = \psi_x(x) \cdot \psi_y(y). \tag{10}$$

$\psi_x(x)$ is a usual potential barrier solution which is split into solutions $\psi_L(x)$, $\psi_B(x)$, and $\psi_R(x)$ for the region on the left side of the barrier, for the barrier region itself, and for the region on the right side of the barrier. $\psi_x(x)$ depends explicitly on the energy $\mathcal{E}$ and, therefore, the two-dimensional solution of Schrödinger equation as denoted as $\psi(x,y;\mathcal{E})$. Electrons are accelerated in the external field $\vec{E}$ parallel to the grain boundary and thus $\psi_y(y)$ is given by the Airy function [10]

$$\psi_y(y) = Ai\Big(\frac{y-\sigma}{\gamma}\Big), \tag{11}$$

where

$$\gamma^3 = \frac{\hbar^2}{2me|\vec{E}|} \text{ and } \sigma = -\frac{\mathcal{E}}{e|\vec{E}|}. \tag{12}$$

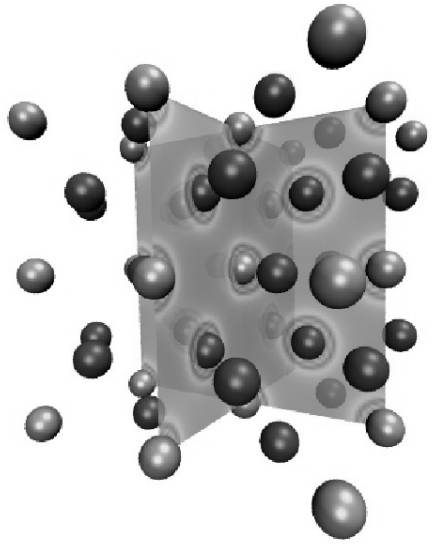

Fig. 1. Portion of the bulk copper crystal. The electron density is represented in two orthogonal planes. It varies from higher values (circle regions around atoms) closer to an atomic nucleus to lower in the inter-atomic space.

The electron density $\rho(\vec{r})$ is easily calculated by integrating over the continuous energy states.

$$\rho(\vec{r}) = \int_0^\infty f(\mathcal{E}-\mathcal{E}_F)DOS(\mathcal{E})|\psi(x,y;\mathcal{E})|^2 d\mathcal{E} \tag{13}$$

Now, the electron wind force is given by a simpler expression [11]

$$\vec{F}(\vec{R}) = -\int \rho(\vec{r})\frac{\partial V(\vec{r}-\vec{R})}{\partial \vec{R}} d^3r \tag{14}$$

which is subsequently used in order to calculate the effective valence.

III. Kinetic Monte Carlo Simulation of Electromigration

To utilize results of quantum mechanical calculations for kinetic Monte Carlo simulations an average driving force along the diffusion jump path must be calculated. In general, the microscopic force-field may depend on the position of the defect along the diffusion jump path. The average of the microscopic force over the j-th diffusion jump path between locations $\vec{r}_{j,1}$ and $\vec{r}_{j,2}$ [3] is

$$F_{m,j} = \frac{1}{|\vec{r}_{j,2} - \vec{r}_{j,1}|}\int_{\vec{r}_{j,1}}^{\vec{r}_{j,2}} \vec{F}(\vec{r}) \cdot d\vec{r}. \tag{15}$$

The change in diffusion barrier height $\Delta A_{\alpha j}$ is equal to the net work by the microscopic force as the defect is moved from initial to final sites over the entire jump path. The rates of defect jumps were calculated using the harmonic

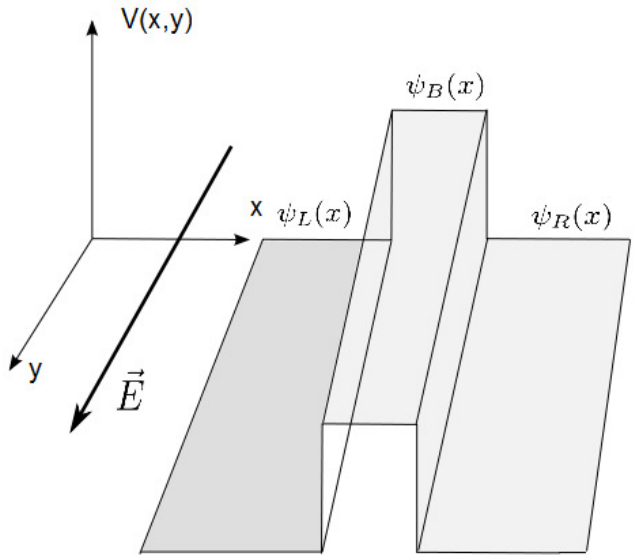

Fig. 2. Grain boundary represented by a two dimensional potential barrier. In order to obtain the effective valence in the copper bulk and the grain boundary an external field oriented parallel to the grain boundary is utilized.

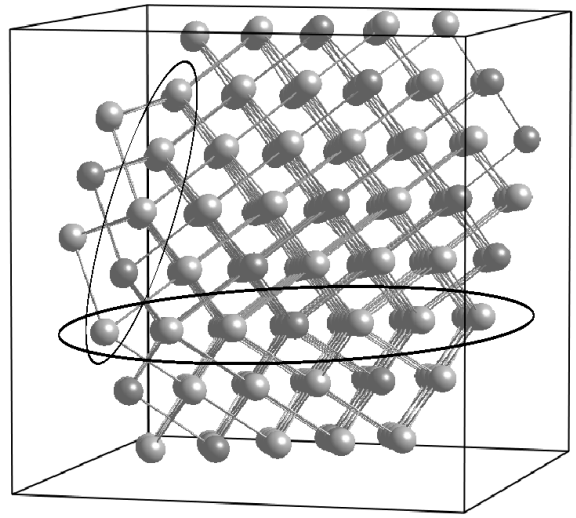

Fig. 3. Formation of grain boundaries (circled regions).

approximation to transition state theory (TST) [12]. In this approximation, the transition rate $\Gamma_{\alpha j}$ is given by

$$\Gamma_{\alpha j} = \nu_0 \exp\Big(-\frac{E_m - \Delta A_{\alpha j}}{kT}\Big). \tag{16}$$

E_m is the migration energy (barrier) defined as the difference in energy between the transition state and the initial state, and ν_0 is an attempt frequency [12]. For each defect site α, the residence time is calculated as [13]

$$\tau_\alpha = \frac{1}{\sum_{j=1}^{k_\alpha} \Gamma_{\alpha j}}. \tag{17}$$

k_α is the number of possible jump sites from the site α. A single point defect is created at an arbitrary site, the clock is set to zero, and the defect is released to walk through the system. At each step, the jump direction is decided by a random number according to the local jump probabilities

$$P_{\alpha j} = \tau_\alpha \Gamma_{\alpha j}. \tag{18}$$

The jump is implemented by updating the coordinates of the defect. By repeating the described random walk procedure for millions of defects, their concentration dependence on the effective valence tensor and the external field is calculated.

IV. Simulation Results

In order to construct atomistic grain boundaries, interfaces, dislocations, and surfaces we apply an in-house molecular dynamic simulator with a multi-body inter-atomic potential [14]. For the construction of the grain boundary a three-dimensional cell with 100 atoms and periodic boundary conditions has been used. Starting with completely disordered atoms in the cell and subsequently reducing the temperature results in the emergence of a realistic grain boundary structure shown in Fig. 3.

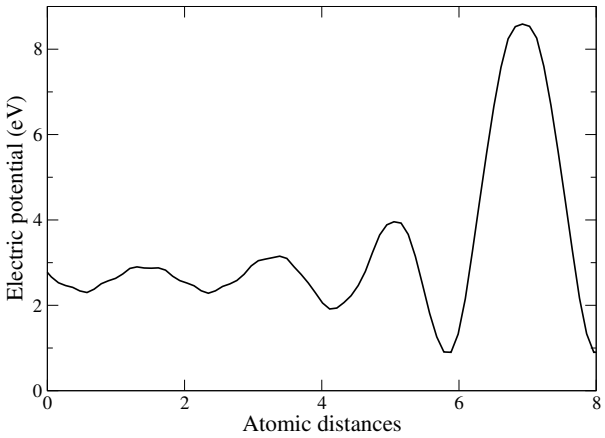

Fig. 4. Electric potential energy in the vicinity of the grain boundary and inside the grain boundary obtained by the density functional theory.

Between two potential methods to calculate the atomistic EM force described in Section II-A and Section II-B, an application of the latter has been presented.

The electric potential inside the bulk and the grain boundary is calculated by means of DFT (cf. Fig. 4). Additionally the Fermi energy has been determined. The one-dimensional distribution of the effective valence is shown in Fig. 5. According to our calculation the effective valence inside the grain boundary is found to be 75% lower than in the bulk for a Fermi energy of 4.3 eV, a value which is in good agreement with the calculation of Sorbello [3].

Calculated values of the effective valence have subsequently

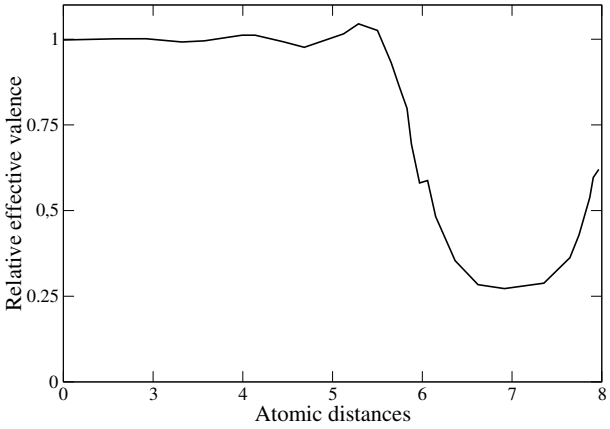

Fig. 5. Average distribution of the effective valence in x-direction near a grain boundary. The external electric field is oriented parallel to the grain boundary.

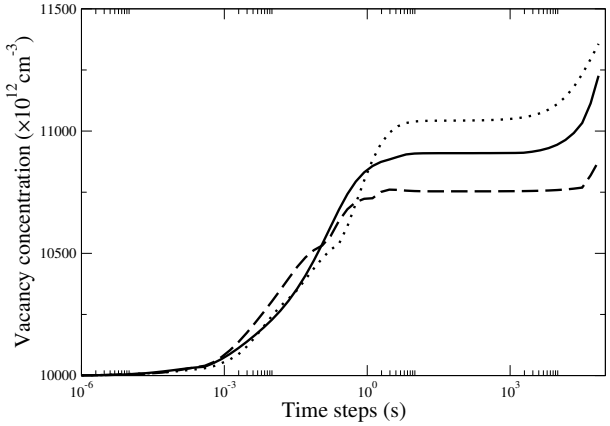

Fig. 6. Variation of the peak vacancy concentration with time for three different microstructures.

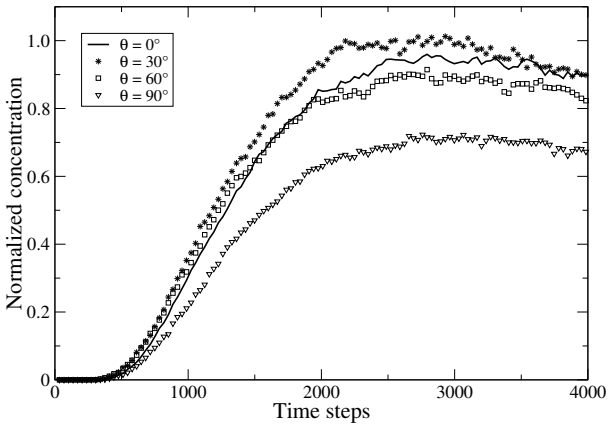

Fig. 7. Concentration difference in control boxes at four different angles (θ) between EM force and atom migration paths.

been included in continuum-level and kinetic Monte Carlo models. In Fig. 6 we show characteristic curves of the EM related vacancy concentration build-up for an extended simulation time. Here a continuum-level EM model is used [15]. All three curves are obtained for the same layout and operating conditions but they differ due to a different copper microstructure.

The calculated atomistic EM force results are also used (see Section III) for kinetic Monte Carlo simulations. This kind of simulation provides a closer look at the migration behavior of atoms. The change in the energy barrier between two equilibrium sites corresponds to the net work by the microscopic EM force. The dependence of the atomic concentration on the angle between the EM force and the jump direction is displayed in Fig. 7.

V. Conclusion

Our work introduces a novel approach for the calculation of the EM force on an atomistic level and demonstrates its application to continuum-level modeling. The consideration of the accurate effective valence in grain boundaries enables a realistic simulation of EM behavior. In addition, the combination of atomistic force calculations with a kinetic Monte Carlo simulation provides sophisticated and quite accurate models for vacancy dynamics inside the grain boundaries.

References

[1] Z.-S. Choi, R. Mönig, and C. V. Thompsona, "Dependence of the Electromigration Flux on the Crystallographic Orientations of Different Grains in Polycrystalline Copper Interconnects," *Appl. Phys. Lett.*, vol. 90, p. 241913, 2007.

[2] E. Zschech and P. R. Besser, "Microstructure Characterization of Metal Interconnects and Barrier Layers: Status and Future," *Proc. Interconnect Technol. Conf*, pp. 233–235, 2000.

[3] R. S. Sorbello, "Microscopic Driving Forces for Electromigration," *Materials Reliability Issues in Microelectronics edited by J. R. Lloyd, F. G. Yost and P. S. Ho*, vol. 225, pp. 3–10, 1996.

[4] R. P. Gupta, "Theory of Electromigration in Noble and Transition Metals," *Phys. Rev. B*, vol. 25, pp. 5188–5196, 1982.

[5] D. N. Bly and P. J. Rous, "Theoretical Study of the Electromigration Wind Force for Adatom Migration at Metal Surfaces," *Phys. Rev. B*, vol. 53, no. 20, pp. 13 909–13 920, 1996.

[6] C. Bosvieux and J. Friedel, "Sur L'electrolyse des Alliages Metalliques," *J. Phys. Chem. Solids*, vol. 23, pp. 123–136, 1962.

[7] P. Kumar and R. S. Sorbello, "Linear-Response Theory of the Driving Forces for Electromigration," *Thin Solid Films*, vol. 25, pp. 25–35, 1975.

[8] R. S. Sorbello, "Pseudopotential-Based Theory on the Driving Forces for the Electromigration in Metals," *J. Phys. Chem. Solids*, vol. 34, no. 6, pp. 937–950, 1973.

[9] G. Kresse and J. Furthmüller, "Efficient Iterative Schemes for *ab initio* Total-Energy Calculations Using a Plane-Wave Basis Set," *Phys. Rev. B*, vol. 54, no. 16, pp. 11 169–11 186, 1996.

[10] R. W. Robinett, *Quantum Mechanics*. Oxford University Press, 1997.

[11] R. S. Sorbello, "Theory of Electromigration," *Solid State Phys.*, vol. 15, pp. 159–231, 1998.

[12] G. H. Vineyard, "Frequency Factors and Isotope Effects in Solid State Rate Processes," *J. Phys. Chem. Sol.*, vol. 3, no. 1, pp. 121–127, 1957.

[13] M. R. Sorensen, Y. Mishin, and A. F. Voter, "Diffusion Mechanisms in Cu Grain Boundaries," *Phys. Rev. B*, vol. 62, no. 6, pp. 3658–3673, 2000.

[14] H. Hakkinen and M. Manninen, "The Effective-Medium Theory Beyond the Nearest-Neighbour Interaction," *J. Phys. Condens. Matter.*, vol. 1, no. 48, pp. 9765–9777, 1989.

[15] H. Ceric, R. L. de Orio, J. Cervenka, and S. Selberherr, "A Comprehensive TCAD Approach for Assessing Electromigration Reliability of Modern Interconnects," *IEEE Trans. Dev. Mat.Rel.*, vol. 9, no. 1, pp. 9–19, 2009.